Nanoparticle Alignment and Repulsion during Failure of Glassy Polymer Nanocomposites

Jong-Young Lee, Qingling Zhang, Todd Emrick, and Alfred J. Crosby*

Polymer Science and Engineering Department, University of Massachusetts, Amherst, Massachusetts 01003

Received May 30, 2006; Revised Manuscript Received August 1, 2006

ABSTRACT: We use a model material of polystyrene blended with surface-modified cadmium selenide nanoparticles to investigate the interaction between polymer molecules and nanoparticles during the process of crazing. We demonstrate that nanoparticles undergo three stages of rearrangement during craze formation and propagation in glassy polymer nanocomposites: (1) alignment along the precraze, (2) expulsion from craze fibrils, and (3) assembly into clusters entrapped between craze fibrils. These results provide insight into the failure mechanisms of glassy polymer nanocomposites.

Introduction

Simulations and experiments of polymer−nanoparticle composites suggest that the similar length scale of nanoparticles and polymer chains can lead to advantageous control of composite mechanical properties.[1−5] Perhaps most significantly, these synergistic length scales play a dominant role in the deformation and failure properties of polymer/nanoparticle composite. Most previous work has focused on the reinforcement mechanism of nanoscale fillers,[1−5] but at these length scales, the mobility of the filler particles, controlled by entropy, can be equally important. In fact, it has been shown that for enthalpically neutral systems conformational entropy of polymer chains can lead to the preferential migration of nanoparticles to cracks, thus leading to a self-healing mechanism for advanced materials.[6−8] Although these results concentrate on the interactions of nanoparticles and polymers in the presence of a crack, many glassy polymer nanocomposites deform first through the onset and propagation of a craze. Crazes, precursor of cracks, are micron-scale regions ahead of a crack tip, where the deformed polymer forms a dense array of nanoscale fibrils (fibril diameter = 5−30 nm).[9,10] For many polymer materials, craze propagation and breakdown define ultimate strength and toughness. These deformation zones in homogeneous materials[11] and microcomposites[12] have been studied extensively. Here, we present the first experimental results on the behavior of well-defined nanoparticles during the onset and propagation of a craze. These results provide understanding of failure mechanism (e.g. crazing) of glassy polymer nanocomposites as well as a new way to alter the spatial distribution of nanoparticles dispersed in a glassy polymer matrix by direct stress and/or strain field.

Because of the large surface-to-volume ratio of nanoparticles, incompatibility between nanoparticles and matrix leads to serious aggregation compared to micron-sized particles. Therefore, the nanoparticle−matrix enthalpic contributions dictate the processing of most conventional nanoscale composites and prevents the composite from fully exploiting possible morphologies. In this work, a model material system was chosen such that entropic factors would be primarily responsible for the behavior of the composites. The polymer matrix is polystyrene (MW = 126K g/mol), and the nanoparticle fillers are polystyrene-modified (MW = 1000 g/mol) cadmium selenide/zinc sulfide (CdSe/ZnS). Because of the existence of grafted short polystyrene chains on the surface of nanoparticles, effects of enthalpic interaction and entanglement between grafted chains and matrix are minimized. The CdSe/ZnS diameter is 5 nm (PS ligand length is 1 nm if fully extended), slightly smaller than the 8 nm radius of gyration (R_g) of the polystyrene. A toluene solution of the polystyrene-grafted nanoparticles and polystyrene homopolymer is cast using a flow-coating process[13] to form thin films (h = 230 nm). Figure 1a,b shows transmission electron microscope (TEM) and optical fluorescence micrographs, which confirms uniform dispersion and photoluminescence of the nanoparticles upon film formation by flow casting. Since our surface-modified nanoparticles are highly compatible with the polystyrene matrix, distribution of nanoparticles through the thickness of the thin films is also uniform.[8] Subsequently, we use the copper grid technique[11] to characterize craze growth. On the basis of previous reports,[13−15] the crazing process and resulting structure is not thickness dependent for polymer thin films over 150 nm in thickness.

Experiment

Synthesis of CdSe Nanoparticles. CdSe/ZnS core/shell nanoparticles were synthesized according to published procedures.[16,17] The synthetic protocol gave CdSe/ZnS nanoparticles covered with tri-*n*-octylphosphine oxide (TOPO) ligands. There TOPO-covered core−shell nanoparticles (∼10 mg) were dissolved in anhydrous pyridine and refluxed under argon for 24 h. Most of the remaining pyridine was removed under vacuum, and hexane was added to precipitate pyridine covered CdSe/ZnS nanoparticles. Anhydrous toluene (∼2 mL) and thiol-terminated polystyrene (∼100 mg, MW = 1300, Polymer Source Inc.) were added to the pyridine-covered nanoparticles. This mixture was heated to 60 °C overnight to give a clear solution. Excess ligands were removed by careful precipitation in hexane.

Preparation of Nanocomposite Thin Film. Polystyrene (M_n = 126K, PDI = 1.02, Polymer Source Inc.) and surface-modified CdSe/ZnS nanoparticles are dissolved in toluene; the volume fraction of CdSe/ZnS is 0.42%. The nanocomposite thin film (230 nm, measured by interferometer, Filmetrics) is cast on silicon oxide substrate by flow coating.[13]

Copper Grid Technique.[11] Crazing is studied using the copper grid technique. In short, this process involves floating and transferring a polymer film onto a copper grid substrate and subsequently

* To whom correspondence should be addressed: e-mail crosby@mail.pse.umass.edu; Tel 413 577-1313; Fax 413 542-0082.

10.1021/ma061210k CCC: $33.50
Published on Web 09/21/2006

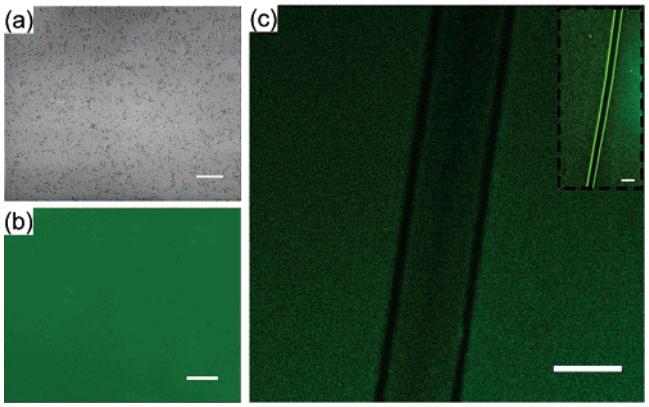

Figure 1. Nanoparticles dispersed in PS matrix (volume fraction of nanoparticles is 0.42%). (a) TEM image (scale bar is 100 nm). (b) Fluorescence image (scale bar is 5 μm). Intensity of fluorescence is uniform. (c) Confocal fluorescence image of the mature craze. Intensity of fluorescence within and outside the craze is uniform. (scale bar is 2 μm). Inset: epifluorescence image of the mature craze (scale bar is 5 μm). Very weak or no fluorescence is observed within the mature craze.

straining the copper grid uniaxially. The copper grid strain is transferred to the polymer film, and because of the low yield strain and plasticity of annealed copper, the copper grid can maintain the applied strain after the sample is unloaded. Transmission electron microscopy (TEM) and fluorescence microscopy are then used to characterize the distribution of nanoparticles.

Transmission Electron Microscopy. We use a razor blade to cut a section from the copper grid. This section is directly mounted into the TEM sample holder. Images are taken by JEOL 2000FX under 200 keV acceleration voltage.

Scanning Confocal Microscopy. The copper grid is fixed on a glass slide by tape. The fluorescence image is taken by a Leica TCS-SP2 confocal microscope. The excitation wavelength is 488 nm, and the emission wavelength between 500 and 550 nm is collected by the photon multiplier tube.

Results

Crazes are narrow (100 nm−2 μm) and long (50−1000 μm) regions of dense arrays of fibrils that grow in length and width with the increase of stress and/or strain.[9,10] A craze can be divided into three regions according to the sequence of craze formation: precraze, premature craze, and mature craze (Figure 2a). The precraze is a locally yielded region (fluidlike) at the leading tip of the craze. Following the precraze, nanofibrils of lower volume fraction form in the premature craze which eventually lead to the formation of the mature craze where nanofibril arrays with a larger volume fraction are found.[11] Crazes grow in width by drawing polymer chains outside the craze into fibrils (surface drawing).[9,11] As the polymer chains are drawn into the fibrils, they align along the extensional axis, creating a highly directed stress field.[9] Fibril breakdown leads to the propagation of a crack behind the craze and subsequent material failure.[10]

The spatial distribution of nanoparticles during craze formation and propagation is altered in polymer nanocomposites. TEM micrographs reveal an assembly and alignment of nanoparticles along the path of the precraze (Figure 3a). Following the precraze region, the premature craze in the nanocomposite is split into multiple, small "secondary crazes" (Figures 2b and 3b). This structure is strikingly different from a conventional premature craze (Figure 2a,c) and has not been observed previously. The secondary crazes form a well-defined path of an "overall" craze and alternate from side to side within this overall craze path. Close inspection of the TEM image shows that no nanoparticles are present within the secondary crazes

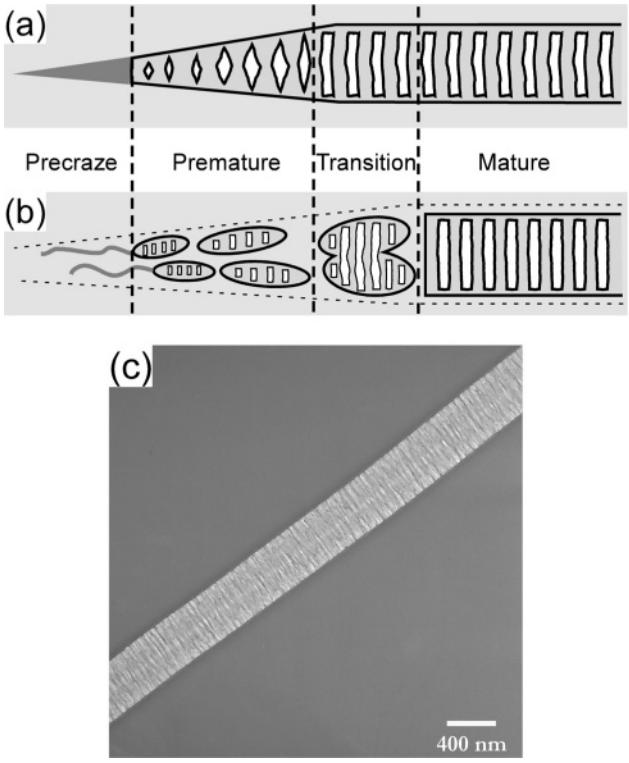

Figure 2. Scheme of craze regions in (a) homopolymer and (b) nanoparticle−polymer composite. Dash line denotes the overall path of the craze. (c) TEM image of premature craze in polystyrene homopolymer (film thickness is 230 nm).

(Figure 3b), even though the regions outside the craze are clearly populated with nanoparticles. This observation implies that the nanoparticles are repelled during the formation of the nanoscale craze fibrils. As the secondary crazes grow in width, they merge to form a transition zone (Figures 2b and 3c). In this zone, the regions between each secondary craze disappear, and nanoparticle clusters are observed in the craze region (Figure 3c). After this merging of secondary crazes, the mature craze forms with its edges clearly aligned in the "overall" craze zone. Here, large cluster bands of nanoparticles are observed near the center (Figure 3d, inset), and smaller clusters are distributed uniformly throughout the mature craze (Figure 3d). The distribution of nanoparticle clusters and bands across the craze width provides a natural "timeline" of how the nanoparticles interact with the craze.

It should be noted that all phenomena described above (i.e., alignment and repellence of nanoparticles, formation of secondary crazes, clustering of nanoparticles) are observed reproducibly for nanocomposites with volume fractions of nanoparticles between 0.31% and 3.3%. When volume fractions are greater than 3.3% (e.g., 14.6%), the crazing process is completely impeded. For low volume fractions (e.g., 0.14%), crazes follow the same growing mechanism as that in polystyrene homopolymer.

Discussion

For nanocomposites with volume fractions within the critical regime, conformational entropy of the polymer chain drives the observations of these experiments, similar to simulations and experiment on the migration of enthalpically neutral nanoparticles to cracks.[6−8] In the PS/CdSe nanocomposites, the rigid, enthalpically neutral interface of the brush-covered nanoparticles limits the conformation of polymer chains in its vicinity. Polymer chains close to nanoparticles are stretched and ex-

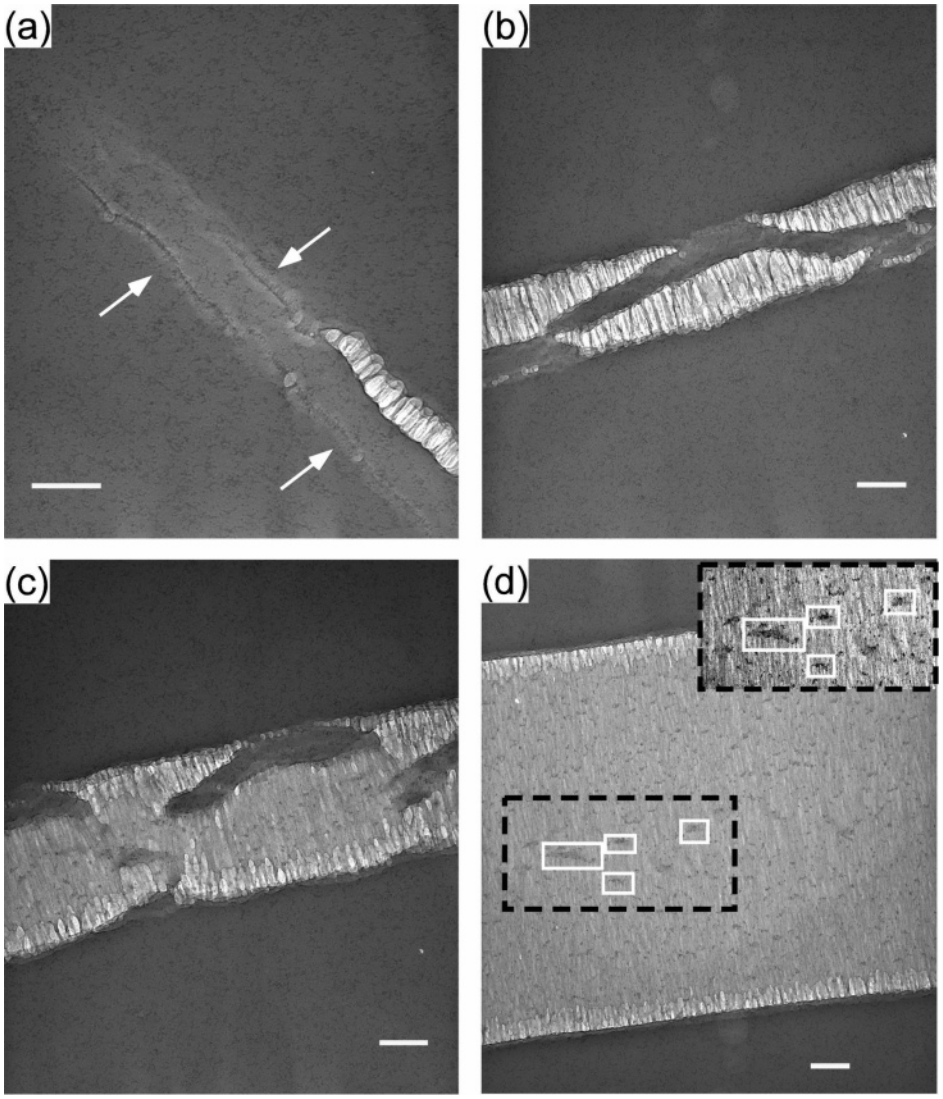

Figure 3. TEM images of the craze regions in polymer nanocompsite (volume fraction of nanoparticles is 0.42%; film thickness is 230 nm): (a) precraze (arrows indicate the alignment of nanoparticles), (b) premature, (c) transition (merging), and (d) mature region. Inset is a magnified image of the black frame. Smaller white frames highlight selected nanoparticle cluster bands located near the center of the mature craze. Scale bars in all figures are 200 nm.

tended, which results in entropy penalty. This decrease in polymer conformational entropy is greater than the decrease in nanoparticle translational entropy; thus, nanoparticle−polymer interactions are minimized by segregation of the nanoparticles. This segregation leads to the alignment of nanoparticles in the precraze region, the repulsion from nanoscale fibrils, and the cluster formation in a mature craze.

In the precraze region, which is fluidlike due to the concentrated stresses that exceed the yield criteria for the matrix, nanoparticles align due to the large gradient of polymer chain mobility in this confined region (Figure 4). At the boundary of the precraze region, the polymer chains are constrained due to the fixation of segments in the uncrazed, glassy matrix, while the chains near the center are highly mobile. This gradient of constraint directs the alignment of nanoparticles, similar to the effect observed in ordered block copolymer matrices where nanoparticles align in the central region of a miscible domain parallel to the microphase boundaries.[18−20] The narrow width of the precraze (∼50 nm), similar to the width of block copolymer microphases, contributes to this alignment process.

While nanoparticle assembly and alignment in the precraze region does not stop the onset of fibril formation in the premature craze, it does alter the structure of the craze

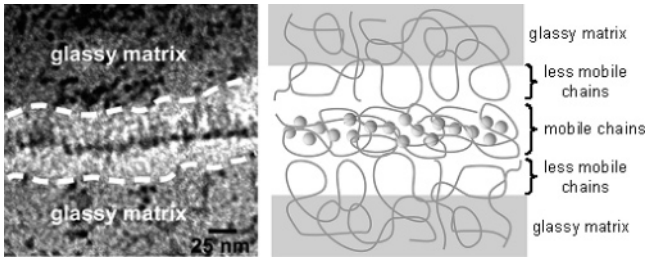

Figure 4. Magnified TEM image of precraze (left) in polymer nanocomposite and corresponding scheme (right). White dash lines in TEM image depict precraze−bulk boundary. Polymer chains in the center are more mobile than chains at the boundary due to fixation of segments in the glassy matrix. Regions with solid gray color (right scheme) represent uncrazed bulk polymer.

significantly. The premature craze in the nanocomposite material consists of a series of alternating secondary crazes. Although the exact origin of this structure is not yet understood, this observation is the first evidence that clearly demonstrates that inorganic filler particles on nanometer length scales impact the growth of a polymer craze. Previous research on the crazing of polymer composites suggested that craze growth mechanism

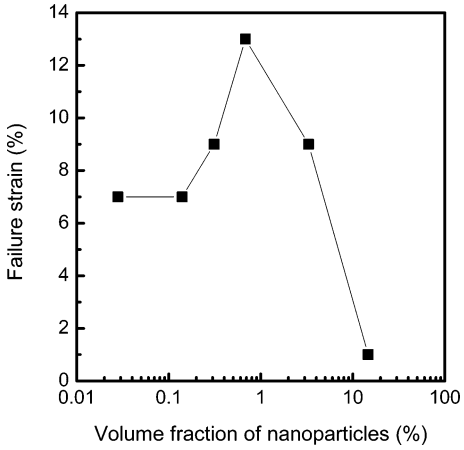

Figure 5. Failure strain of nanocomposites as a function of volume fraction of nanoparticles.

are not influenced by fillers of submicron dimensions.[12] Our results contradict this conclusion definitively.

In addition to causing the onset of secondary craze structures, nanoparticles are repelled from the craze nanofibrils within these secondary crazes. This mechanism is directly related to the conformational entropy of the polymer molecules. As the craze fibrils grow, polymer molecules from the surrounding region are drawn into the fibril and subsequently stretched and aligned. The fibril volume is highly confined (diameter = 5−30 nm); therefore, the presence of a 5 nm particle within a fibril will significantly decrease the conformational entropy of a polymer chain. This repulsion is similar to the "depletion attraction" phenomenon described by Balazs et al.[6,7,21,22]

For mature crazes, the repulsion during fibril growth in length leads to nanoparticle entrapment between craze fibrils. This entrapment begins as the material between the secondary crazes is drawn completely into the craze fibrils (merging of secondary crazes) and one continuous craze structure is formed (mature craze). During this merging process, the repelled nanoparticles from secondary crazes are entrapped between the newly formed fibrils and are observed as large cluster bands close to the center of the mature craze (Figure 3d, inset). The newly formed mature crazes continue to grow in width as polymer chains are drawn into fibrils, and nanoparticles are repelled from the confines of the nanofibrils. The distribution of nanoparticle clusters throughout the craze width (Figure 3d) implies that nanoparticles are initially repelled, assembled at the edge of the craze, and eventually surpassed and entrapped by the growing craze fibril network/array. The polymer chains forming the nanofibrils follow the path of least resistance and grow around regions of sequestered nanoparticles. Since nanoparticles do not stay within craze fibrils, they cannot strengthen craze fibrils directly. This trapping of nanoparticles would also occur in the premature region if the extent of fibril growth was sufficient prior to the merging of the "secondary crazes". These entrapped nanoparticles decrease the number of cross-tie fibrils, consequently impeding the growth of a crack. However, the buildup of nanoparticles in the craze−bulk boundary impedes craze widening, consequently facilitating material failure. These two effects lead to an optimal volume fraction of nanoparticles (Figure 5) at which the failure strain increases to a maximum value, ~90% greater than homopolymer PS. More details will be given in a subsequent publication.

Although nanoparticles form aggregated clusters within mature craze, the nanoparticles do not coalesce, and their fluorescent properties are not compromised. This observation

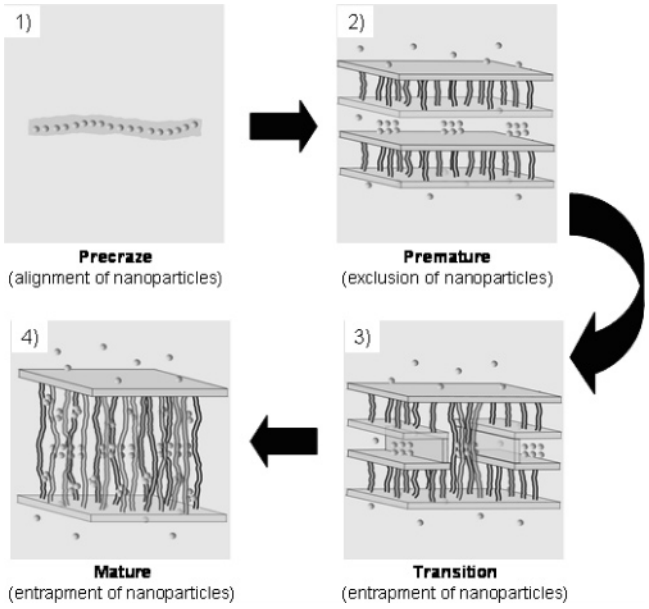

Figure 6. Summary of the interaction between polymer molecules and nanoparticles during crazing process. (1) Nanoparticles are aligned and assembled along the precraze. (2) Premature region consists of several secondary crazes (two are shown in the scheme). Nanoparticles are repelled from secondary crazes during the formation of nanofibrils. (3) Merging of secondary crazes (transition region). Nanoparticles are trapped within the crazed region during merging process. (4) Within mature craze, larger cluster bands of nanoparticles are observed near the center of the craze, and smaller clusters are distributed uniformly within the mature craze.

is confirmed by the uniformity of nanoparticle fluorescence both within and outside the mature craze region (Figure 1c). Scanning confocal microscopy is used for these images to avoid geometric effects since a craze is a depressed region on the surface of the material.[23] By conventional reflected light fluorescence microscopy, very weak or no fluorescence is observed within the mature craze region (Figure 1c, inset), and this observation alone may cause misinterpretation of nanoparticle distribution within mature craze. Fluorescence both within and outside the craze is in direct agreement with high-resolution TEM of the mature craze region (Figure 3d), where nanoparticle clusters are distributed throughout the region. The two narrow dark bands along the edges of the mature craze in the scanning fluorescence micrograph are not due to the loss of fluorescence, but rather attributed to optical effects that result from inclination of the craze edge. Further evidence that these bands are produced optically is provided by scanning reflection mode microscopy where only excitation and not emission light is collected by the detector. Under this mode, the same dark bands are observed.

Conclusion

Figure 6 qualitatively summarizes the four primary mechanisms of polymer−nanoparticle composite behavior with respect to crazing: (1) nanoparticles align in the precraze; (2) premature crazes advance through "secondary" crazes and nanoparticles are repelled from craze fibrils; (3) secondary crazes merge to form mature craze; and (4) nanoparticles are entrapped by the craze fibril array in a mature craze. In addition to demonstrating the alignment and change in spatial distribution of nanoparticles in a glassy polymer matrix, these experimental results provide direct evidence that nanoscale particles do not prevent the formation of nanoscale fibrils, nor do they provide enhanced strength by the reinforcement of the fibrils. However, alignment, formation of secondary crazes and repulsion of nanoparticles

leads to the formation of new craze microstructures with nanoparticle clusters entrapped within mature craze. This "self-assembled" microstructure is the key mechanism for enhancing the deformation and failure properties in these materials and is clearly linked to the unique size-scale dependent, entropically driven mobility provided by the interfacially tuned nanoparticles.

Acknowledgment. Funding for this project is provided by the NSF-MRSEC at the University of Massachusetts, Petroleum Research Fund of the American Chemical Society, and the Department of Energy (DE-FG-02-96ER45).

References and Notes

(1) Buxton, G. A.; Balazs, A. C. *J. Chem. Phys.* **2002**, *117*, 7649−7658.
(2) Thio, Y. S.; Argon, A. S.; Cohen, R. E.; Weinberg, M. *Polymer* **2002**, *43*, 3661−3674.
(3) Wilbrink, M. W. L.; Argon, A. S.; Cohen, R. E.; Weinberg, M. *Polymer* **2001**, *42*, 10155−10180.
(4) Koerner, H.; Liu, W. D.; Alexander, M.; Mirau, P.; Dowty, H.; Vaia, R. A. *Polymer* **2005**, *46*, 4405−4420.
(5) Thostenson, E. T.; Li, C. Y.; Chou, T. W. *Comput. Sci. Technol.* **2005**, *65*, 491−516.
(6) Lee, J. Y.; Buxton, G. A.; Balazs, A. C. *J. Chem. Phys.* **2004**, *121*, 5531−5540.
(7) Tyagi, S.; Lee, J. Y.; Buxton, G. A.; Balazs, A. C. *Macromolecules* **2004**, *37*, 9160−9168.
(8) Gupta, S.; Zhang, Q. L.; Emrick, T.; Balazs, A. C.; Russell, T. P. *Nat. Mater.* **2006**, *5*, 229−233.
(9) Kramer, E. J. *Adv. Polym. Sci.* **1983**, *52*−*3*, 1−56.
(10) Kramer, E. J.; Berger, L. L. *Adv. Polym. Sci.* **1990**, *91*/*91*, 2−68.
(11) Lauterwasser, B. D.; Kramer, E. J. *Philos. Mag. A* **1979**, *39*, 469−495.
(12) Donald, A. M.; Kramer, E. J. *J. Appl. Polym. Sci.* **1982**, *27*, 3729−3741.
(13) Lee, J.-Y.; Crosby, A. J. *Macromolecules* **2005**, *38*, 9711−9717.
(14) Donald, A. M.; Chan, T.; Kramer, E. J. *J. Mater. Sci.* **1981**, *16*, 669−675.
(15) Chan, T.; Donald, A. M.; Kramer, E. J. *J. Mater. Sci.* **1981**, *16*, 676−686.
(16) Skaff, H.; Emrick, T. *Angew. Chem., Int. Ed.* **2004**, *43*, 5383−5386.
(17) Sill, K.; Emrick, T. *Chem. Mater.* **2004**, *16*, 1240−1243.
(18) Thompson, R. B.; Ginzburg, V. V.; Matsen, M. W.; Balazs, A. C. *Science* **2001**, *292*, 2469−2472.
(19) Lee, J. Y.; Thompson, R. B.; Jasnow, D.; Balazs, A. C. *Phys. Rev. Lett.* **2002**, 89.
(20) Bockstaller, M. R.; Lapetnikov, Y.; Margel, S.; Thomas, E. L. *J. Am. Chem. Soc.* **2003**, *125*, 5276−5277.
(21) Huh, J.; Ginzburg, V. V.; Balazs, A. C. *Macromolecules* **2000**, *33*, 8085−8096.
(22) Lee, J. Y.; Shou, Z.; Balazs, A. C. *Phys. Rev. Lett.* **2003**, *91*, 136103.
(23) Yang, A. C. M.; Kunz, M. S.; Logan, J. A. *Macromolecules* **1993**, *26*, 1767−1773.

MA061210K